JPEDAV (2008) 29:390–397
DOI: 10.1007/s11669-008-9356-2
1547-7037 ©ASM International

Calculation of Two-Dimensional Sections of Liquidus Projections in Multicomponent Systems

Shuanglin Chen, Ying Yang, Weisheng Cao, Bernard P. Bewlay, Kuo-Chih Chou, and Y. Austin Chang

(Submitted March 26, 2008; in revised form May 28, 2008)

A two-dimensional (2D) section of liquidus projection consists of univariant lines of three-phase equilibria between liquid and other phases. It is useful not only for people's easy visualization but also for retaining important information about the multicomponent liquidus surface, which is critical for understanding and controlling the solidification microstructure. An algorithm is presented for calculating two-dimensional sections of liquidus projections for multicomponent systems. It can project a liquidus surface onto any given two-dimensional section in the compositional space. A hypothetical quaternary system is designed to illustrate the features of the 2D sectional liquidus projections. Then the Nb-Ti-Si-Cr system is used as an example to demonstrate how to apply a 2D sectional liquidus projection to determine the amount of Cr addition into Nb-Ti-Si alloy to affect the liquidus surface of the quaternary system.

Keywords computational studies, equilibrium diagram, invariant equilibria, liquidus surface, phase diagram, phase equilibria

1. Introduction

A liquidus projection diagram is a special phase diagram. It displays the phase relationships between a liquid phase and other phases (including the liquid phase itself if the liquid exhibits a miscibility gap) in the system.[1] The information provided by a liquidus projection is very important for understanding and controlling the solidification microstructure.

In principle, a phase diagram of an n-component system can be calculated in the n dimensional (nD) composition-temperature space as long as the thermodynamic functions of phases in the system are known. The authors have implemented an algorithm to calculate the liquidus projection for an n-component ($n \geq 3$) system, in which the nD univariant reaction lines in the nD composition-temperature space are calculated. However, these univariant lines cannot be drawn and visualized if n is greater than 4. In fact, when $n = 4$, the diagram becomes very complicated and hard to visualize. The present paper describes an algorithm that calculates the 2D sectional liquidus projections of n-component systems ($n \geq 4$). In the following, the authors only consider phase equilibria for a system at constant pressure in the composition-temperature state space. Before introducing the calculation of 2D sections of a liquidus projection, the general features of 2D sectional phase diagrams in composition-temperature space and 2D sectional liquidus projection diagrams in compositional space are presented.

Shuanglin Chen, Ying Yang, and **Weisheng Cao**, CompuTherm, LLC, Madison, WI 53719; **Shuanglin Chen** and **Kuo-Chih Chou**, School of Materials Science and Engineering, Shanghai University, Shanghai 200072, China; **Bernard P. Bewlay**, General Electric Co., GE Global Research Center, Niskayuna, NY 12309; **Kuo-Chih Chou**, Department of Physical Chemistry, University of Science and Technology Beijing, Beijing 100083, China; and **Y. Austin Chang**, Department of Materials Science and Engineering, University of Wisconsin, Madison, WI 53706. Contact e-mail: chen@chorus.net.

2. Phase Diagrams and 2D Sectional Phase Diagrams

For an n-component system, the composition-temperature space, (x_1, x_2, x_3, …, x_{n-1}, T), is an n-dimensional (nD) space. In a phase diagram in an nD space, there exist different dimensional geometric objects: 0D points (invariant), 1D lines (univariant curves), 2D planes (divariant surfaces), and so on. To fully calculate all these geometric objects for a large n is almost impossible and also unnecessary. Usually, calculation is performed in a space with number of dimensions less than 4, for example, a specific 2D section of a phase diagram in the nD space.

A 2D sectional phase diagram consists of phase boundaries (univariant 1D lines in the 2D space), which separate adjacent phase fields. A phase field in the 2D section contains the number of phases ranging from 1 to $n + 1$. Some phase fields may degenerate into 1D lines or 0D points. Calculations are carried out point by point, that is, a line of consecutive points, for each univariant line. Figure 1 is a typical 2D sectional phase diagram, an isoplethal section of the Al-Cu-Mg-Si quaternary, in which the concentrations of Al and Si are fixed at 60 and 8 wt.%, respectively.

However, 2D sectional liquidus projections are significantly different from 2D sections of composition-temperature phase diagrams, which are discussed in the next section.

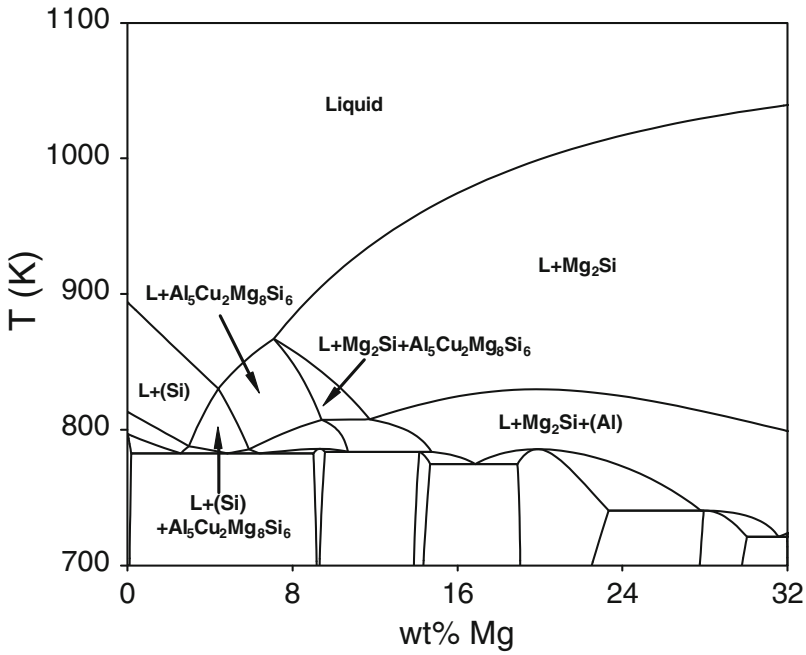

Fig. 1 A calculated isopleth of Cu-Mg for Al-Cu-Mg-Si at 60 wt.% Al and 8 wt.% Si

3. Liquidus Projection and 2D Sectional Liquidus Projection

In order to formulate an algorithm to calculate a 2D sectional liquidus projection, the features of 2D sectional liquidus projections are presented below.

3.1 Liquidus Projection

Conventionally, a liquidus projection refers to a ternary liquidus projection, in which the liquidus surface is projected along the temperature direction onto the 2D compositional plane of (x_1, x_2). Figure 2 shows an example of the liquidus projection of Nb-Ti-Si ternary.

A ternary liquidus surface has 2D divariant surfaces of two-phase equilibria, 1D univariant lines of three-phase equilibria, and 0D invariant points of four-phase equilibria. In a ternary liquidus projection as shown in Fig. 2, the solid lines represent the liquid compositions involved in univariant three-phase equilibria. The areas enclosed by the univariant lines and the sides of the compositional triangle represent the set of liquid compositions associated with divariant two-phase equilibria. Three univariant lines intersect at a four-phase invariant point.

An n-component liquidus surface has $(n-1)$D hypervolumes of two-phase equilibria, …, 2D divariant surfaces of $(n-1)$-phase equilibria, 1D univariant lines of n-phase equilibria, and 0D invariant points of $(n+1)$-phase equilibria. The algorithm calculating liquidus projections presented in Ref [2] calculates only the 1D univariant lines of n-phase equilibria and the 0D invariant points of $(n+1)$-phase equilibria (intersections of 1D lines) for an n-component system. In the following, the features of liquidus projection

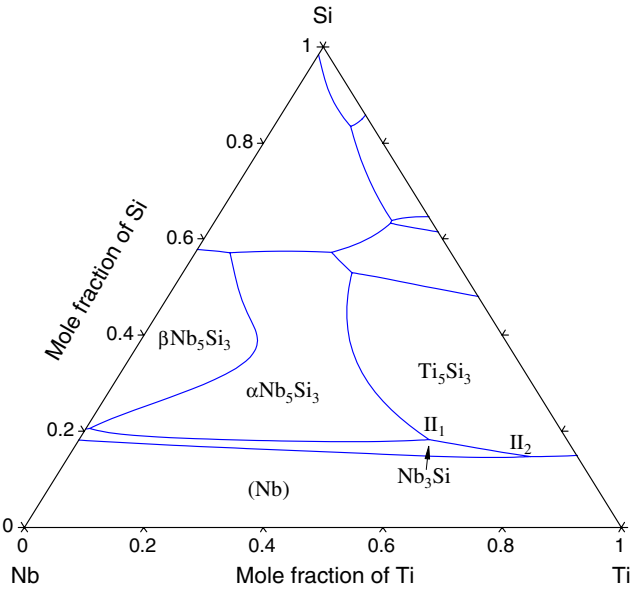

Fig. 2 Calculated liquidus projection for ternary Nb-Ti-Si

and 2D sectional liquidus projection are discussed using a hypothetical A-B-C-D quaternary system.

A quaternary liquidus surface is composed of 3D volumes in a 4D space of (x_1, x_2, x_3, T) and *is nearly impossible to view directly*. Similar to a ternary liquidus projection, a quaternary liquidus projection can be projected onto a 3D space of (x_1, x_2, x_3) along the temperature direction. Assume that a hypothetical quaternary system has five phases: liquid, α, β, γ, and δ. All five phases are assumed to be ideal solution phases. The entropies of melting are set to be 10 J/K per mole of atoms for every

component in each phase. Also, the melting temperatures for components in each phase are listed in Table 1. If the liquid phase is taken as the reference phase, the Gibbs energy of the components j in the phase φ is represented by

$$G_j^{\varphi} = G_j^{liquid} - (T_m^{\varphi} - T)S_{m,j}^{\varphi} \quad (\varphi = \alpha, \beta, \gamma, \delta)$$

where T_{m}^{φ} and $S_{\mathrm{m},j}^{\varphi}$ are the temperature of the melting point and the entropy of melting of component j in phase φ, respectively.

Table 1 The melting temperatures (in K) of components for the phases in a hypothetical quaternary system A-B-C-D

	Temperature, K			
Phase	**A**	**B**	**C**	**D**
α	1000	100	110	120
β	200	900	250	300
γ	150	160	800	170
δ	300	310	320	700

Figure 3 is the quaternary liquidus projection tetrahedron for the hypothetical A-B-C-D system calculated by Pandat.[2] In Fig. 3, "e_i" (i = 1, 2, …, 6) denotes invariant eutectic reactions in the constituent binaries, while "I_i" (i = 1, 2, 3, 4) denotes those in ternaries. "I_{q5}" is the invariant (five-phase) eutectic reaction in the quaternary. Table 2 lists the temperatures and compositions for these special points. The gray lines in both dotted and solid denote the univariant three-phase equilibria in the constituent ternaries. The dark thick lines denoted by "I_i-I_{q5}" (i = 1, 2, 3, 4) represent the univariant four-phase equilibria in the quaternary. These "I_i-I_{q5}" (i = 1, 2, 3, 4) lines divide the tetrahedron into four volumes, that is, the primary solidification regions of α, β, γ, and δ. At the intersection of two such volumes is a three-phase equilibrium interface. At the intersection of three such volumes is a four-phase equilibrium interface, as denoted by "I_i-I_{q5}" (i = 1, 2, 3, 4). "I_{q5}" is the intersection of the four volumes, representing the invariant five-phase equilibrium.

In a similar way, the liquidus surfaces in an n-component system can be projected onto an $(n-1)$D compositional

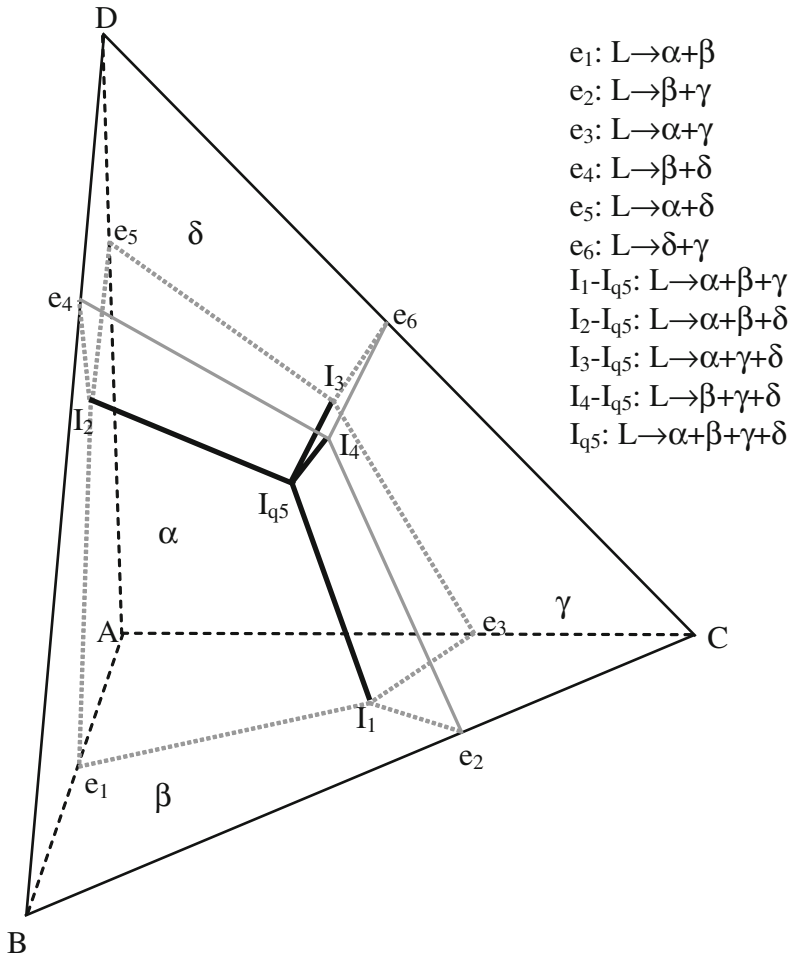

Fig. 3 Schematic tetrahedron showing a calculated liquidus projection of a hypothetical A-B-C-D quaternary system. The gray line denotes the univariant lines in the constituent ternaries; the thick dark line denotes the univariant lines in the quaternary. The reactions denoted by e_i and I_i are shown in the legend

Table 2 The compositions and temperatures for the invariant points in the hypothetical quaternary system

Reaction	Symbol	T, K	x_A	x_B	x_C	x_D
$L \rightarrow \alpha + \beta$	e_1	679.0	0.456	0.544		
$L \rightarrow \beta + \gamma$	e_2	619.8		0.415	0.585	
$L \rightarrow \alpha + \gamma$	e_3	632.7	0.384		0.616	
$L \rightarrow \beta + \delta$	e_4	596.1		0.347		0.653
$L \rightarrow \alpha + \delta$	e_5	598.9	0.333			0.667
$L \rightarrow \gamma + \delta$	e_6	561.7			0.460	0.540
$L \rightarrow \alpha + \beta + \gamma$	I_1	546.5	0.266	0.298	0.436	
$L \rightarrow \alpha + \beta + \delta$	I_2	537.7	0.253	0.266		0.481
$L \rightarrow \alpha + \gamma + \delta$	I_3	513.9	0.222		0.370	0.408
$L \rightarrow \beta + \gamma + \delta$	I_4	514.3		0.226	0.369	0.405
$L \rightarrow \alpha + \beta + \gamma + \delta$	I_{q5}	480.6	0.184	0.186	0.310	0.320

space (x_1, x_2, x_3, …, x_{n-1}). However, it cannot be plotted if $n > 4$. To better view a multicomponent liquidus surface information, the authors choose 2D sections of liquidus projections. Even though a lot of information will be lost after projection, 2D sections of liquidus projection still assist in understanding the liquidus surfaces.

There are two methods of generating a 2D sectional liquidus projection. The first method is "section of projection," which projects the liquidus surface onto compositional space and then takes a 2D section of the projection. The second method is "projection of sections," which takes a series of 2D sections of the liquidus surface in composition-temperature space to form a 3D liquidus surface and then projects the 3D liquidus surface onto a 2D plane. The 2D sectional liquidus projections generated from these two methods are identical. These two methods are explained with examples below.

3.2 Section of Projection

Here the authors use the quaternary example above to illustrate how this method works. In the tetrahedron in Fig. 3, the lines denoted by I_1-I_{q5}, I_2-I_{q5}, I_3-I_{q5}, and I_4-I_{q5} are the projections of the quaternary univariant phase equilibria in the compositional space. Between two adjacent univariant lines there is a surface of three-phase equilibria. When a 2D plane passes through this 3D tetrahedron, it cuts the surfaces of these three-phase equilibria and the intersections will be lines on the 2D plane. These lines on the 2D sectional plane represent three-phase equilibria, and they cross at four-phase equilibrium invariant points. Several 2D sections are calculated to illustrate the basic features of such diagrams.

Figure 4(a) shows two 2D sections parallel to the A-B-C face in the tetrahedron, and Fig. 4(b) and (c) are the details of the liquidus projections on the 2D sections. Figure 4(b) from Section (I) is defined by three points (Y:0.8A-0.2D)-(O:0.8B-0.2D)-(X:0.8C-0.2D) with x_D = 0.2, which is below I_{q5}, where Y, O, and X denote *Y*-axis, origin, and *X*-axis, respectively. It cuts a point on the univariant line I_1-I_{q5}. This section consists of the primary phases α, β, and γ. The numerals "1" through "5" in Fig. 4(b) will be used in next section. Figure 4(c) from Section (II) is the liquidus projection on another 2D section of (Y:0.65A-0.35D)-(O:0.65B-0.35D)-(X:0.65C-0.35D) with x_D = 0.35 just above I_{q5}. This section consists of a small δ primary phase region surrounded by the primary phase regions of α, β, and γ. Unlike Fig. 4(b) cutting through only one univariant line I_1-I_{5q}, this section cuts through the other three univariant lines: I_2-I_{q5}, I_3-I_{q5}, and I_4-I_{q5}. The cutting points are those intersection points in Fig. 4(c).

It is possible to define a 2D section to exactly pass through the invariant point I_{q5}. Section (III) in Fig. 5(a) is one of such sections, which is parallel to both edges of AB and CD in the tetrahedron. Figure 5(b) shows the details of the liquidus projection on the 2D Section (III). The 2D section cutting right through I_{q5}, as in Fig. 5(a) and (b), is defined by (Y:0.37B-0.63D)-(O:0.37B-0.63C)-(X:0.37A-0.63C) and has four primary phases intersecting at one point, I_{q5}. Other types of topology could be obtained from different 2D sections. With the aid of different 2D sections, we can better understand the liquidus projections in multicomponent systems, which are difficult to visualize in high-dimensional space.

3.3 Projection of Sections

Besides the method of section of projection, 2D sectional liquidus projection can also be obtained by the method of projection of sectional phase diagrams. Here the sectional phase diagrams refer to isopleths, as shown in Fig. 1. By calculating a series of isopleths in the composition-temperature space of (x_1, x_2, x_3, …, x_{n-1}, T), we can obtain the compositions and temperatures of three-phase equilibria involving liquid and two other phases. These three-phase equilibria can then be projected onto a 2D compositional plane. We demonstrate here how this method is applied to construct the 2D sectional liquidus projection in Fig. 4(b). Figure 6(a-d) are four isoplethal sections of A-B-C-D with the composition of D being fixed at 0.2 and that of C varying from 0.1 to 0.4. The points denoted by numerals 1-5 in Fig. 4(b) correspond to the points denoted by the same numerals in Fig. 6(a-d). We can also calculate many other isopleths, from which a whole 2D sectional liquidus projection as shown in Fig. 4(b) can be constructed. This confirms that the section of projection and the projection of sections are equivalent in constructing a 2D sectional liquidus projection.

4. Computational Algorithm

It can be seen from above discussion that a 2D sectional liquidus projection consists of univariant lines of three-phase equilibria among liquid and two other phases. Three univariant lines meet at one invariant point. An algorithm to calculate a 2D sectional liquidus projection is presented below. The algorithm includes four major steps.

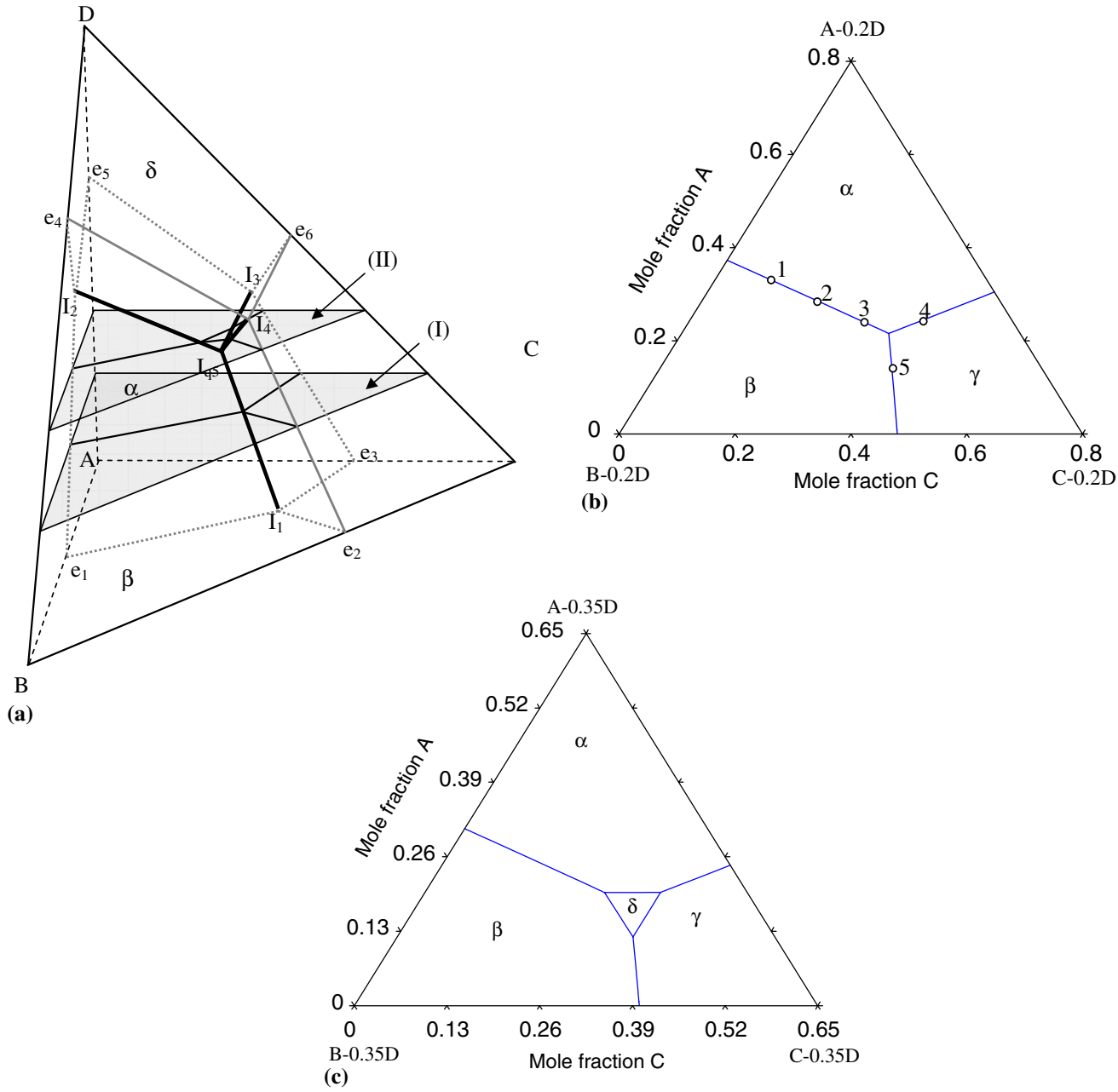

Fig. 4 Calculated liquidus projection on the 2D sections paralleling to the face of A-B-C in tetrahedron. (a) 2D sections (I) and (II) in the tetrahedron of quaternary liquidus projection. See (b) and (c) for details. (b) Section of (Y:0.8A-0.2D)-(O:0.8B-0.2D)-(X:0.8C-0.2D). Numerals "1" through "5" correspond to the invariant points in Fig. 6. (c) Section of (Y:0.65A-0.35D)-(O:0.65B-0.35D)-(X:0.65C-0.35D)

4.1 Definition of the Coordinate System

To calculate a 2D section, first step is to define a 2D coordinate system. The 2D section is in the compositional space of (x_1, x_2, x_3, …, x_{n-1}). In a Cartesian coordinate system, there are two major different methods to define a 2D plane: define an origin point and two directions from the origin to form a 2D plane and define three noncollinear points in the coordinate system to construct a plane passing through the three points. Mathematically, these two methods are equivalent. However, the second method is more flexible to use than the first one. Pandat[3,4] adopts the second method. This method is used here for defining a 2D section. Figure 5 is an example showing that it is not necessary to fix some components at constant compositions for a 2D section. Any three noncollinear points can define a 2D section. In the hypothetical quaternary system in Fig. 3, the coordinate system is (x_A, x_B, x_C, x_D). Let three noncollinear points be expressed as:

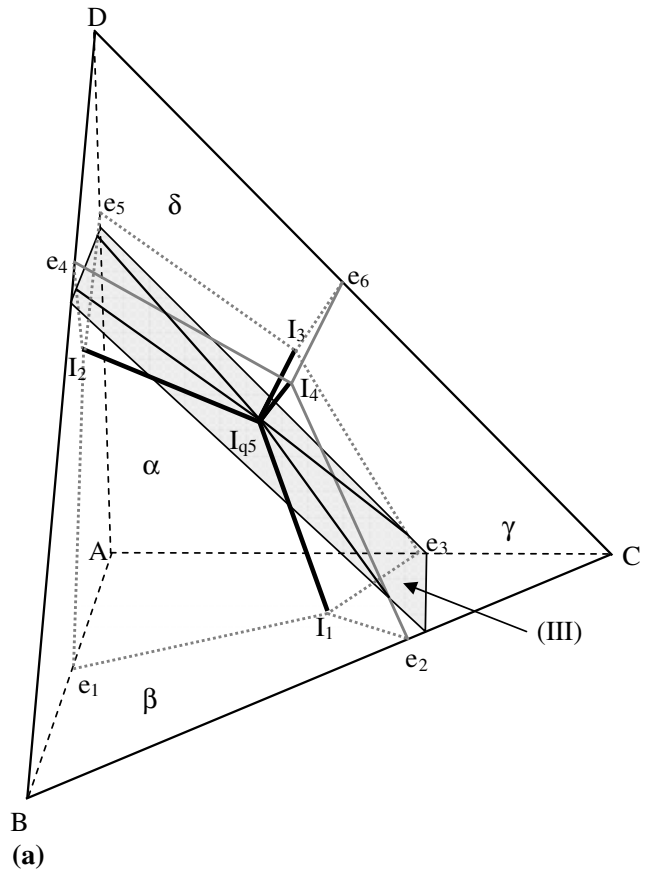

(a)

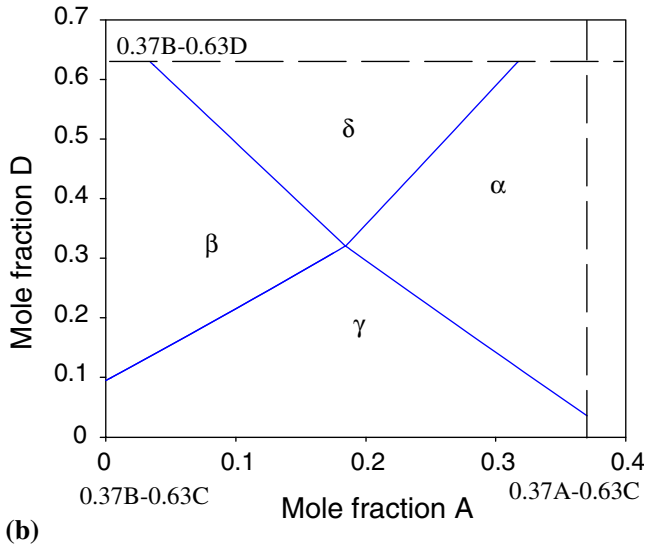

(b)

Fig. 5 Calculated liquidus projection on a 2D section that parallels to the edges of AB and CD in tetrahedron of the quaternary liquidus projection. (a) 2D section (III) in the tetrahedron of the quaternary liquidus projection. See (b) for details. (b) Section of (Y:0.37B-0.63D)-(O:0.37B-0.63C)-(X:0.37A-0.63C)

$$(x_A^{(i)}, x_B^{(i)}, x_C^{(i)}, x_D^{(i)}) \quad (i = 1, 2, 3)$$

where the superscripts in the parentheses are the indices of points. For example, the section of Fig. 4(a) is defined by the three points of (0.8, 0, 0, 0.2), (0, 0.8, 0, 0.2), and (0, 0, 0.8, 0.2) and the section of Fig. 5(b) is defined by (0, 0.37, 0, 0.63), (0, 0.37, 0.63, 0), and (0.37, 0, 0.63, 0). None of the components in Fig. 5(b) is kept as a constant.

4.2 Set Scan Lines

After the coordinate system is defined for the 2D section, a few scan lines are placed within the coordinate system. Along these scan lines, the liquidus surface temperatures will be calculated for the points on the scan lines in certain intervals, for example, 100 points for each scan line. If two neighbor points on a scan line have different primary phases in equilibrium with liquid, a three-phase equilibrium among liquid phase and the two primary phases must exist between the two points on the liquidus surface. This three-phase equilibrium will be calculated and used as a starting point for the calculation of the univariant line in the 2D section in next step.

4.3 Calculation of Univariant Phase Equilibria

After the calculations on the scan lines are done, calculation will start from all the starting points to calculate the univariant lines with three-phase equilibria. For the connected univariant lines, one starting point will be enough. Duplicate calculations could be avoided by examining whether the univariant line represented by a remaining starting point has been calculated or not.

4.4 Calculation of Invariant Phase Equilibria

After calculation of each univariant equilibrium point, its global stability of the equilibrium is verified. If there is another phase becoming more stable, a four-phase invariant equilibrium will be calculated. Since three univariant lines meet at one invariant point, two new univariant lines will be calculated recursively from this invariant point.

Calculation is finished when each univariant line ends on the edge of the coordinate system or at an invariant point and all starting points have been considered. The calculation results will then be plotted.

This algorithm has been implemented in Pandat and used for the calculations of above 2D sectional liquidus projections of the hypothetical quaternary system. Quaternary Nb-Ti-Si-Cr will be taken as an example in the next section to demonstrate how to use the 2D sectional liquidus projections in alloy design.

5. 2D Sectional Liquidus Projections for Nb-Ti-Si-Cr System

Nb-Si-based refractory metal intermetallic composites (RMICs) are potential candidates for the next generation of high-temperature structural materials.[5–8] Nb-Si-based RMICs are typically alloyed with Cr and Ti for improved balance of materials properties.[5, 6] The fabrication of components of these alloys usually involves solidification

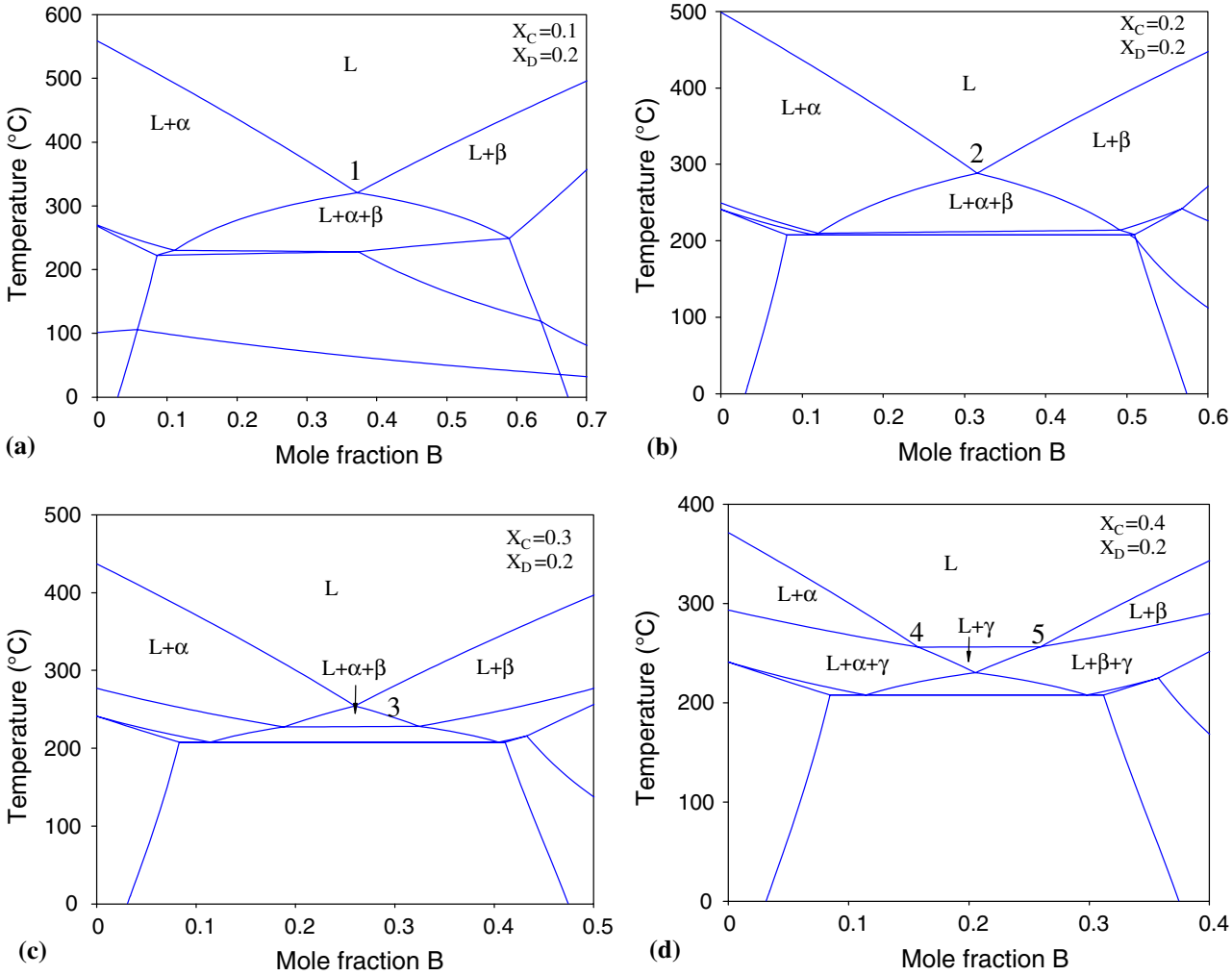

Fig. 6 Calculated isopleths of A-B-C-D with x_D = 0.2 and (a) x_C = 0.1, (b) x_C = 0.2, (c) x_C = 0.3, and (d) x_C = 0.4. Numerals "1" through "5" correspond to those in Fig. 4(b)

processing. The liquid-solid phase equilibria data are required to understand the microstructure and the properties. Figure 2 is the liquidus projection of the Nb-Ti-Si ternary system. In the metal-rich region, there are five primary phases, βNb_5Si_3, αNb_5Si_3, Nb_3Si, Ti_5Si_3, and (Nb). The preferred constituent phases in these alloys are (Nb) and αNb_5Si_3. The phase (Nb) is needed for ductility and fracture toughness, and the intermetallic αNb_5Si_3 is required for high-temperature creep strength and oxidation resistance. In the Nb-Ti-Si ternary system, there is no direct solidification reaction between (Nb) and αNb_5Si_3 for the Nb-rich Nb-Ti-Si alloys. The eutectic reaction is between (Nb) and Nb_3Si. The Nb_3Si decomposes into (Nb) and αNb_5Si_3 via a eutectoid reaction at high temperature (~1700 °C). However, the decomposition kinetics are very sluggish. Therefore, the Nb_3Si is always present in the as-cast alloys. However, experiments have shown that with addition of Cr to the Nb-Ti-Si system, it is possible to form a direct eutectic between (Nb) and αNb_5Si_3.

The 3D liquidus projection of the quaternary Nb-Ti-Si-Cr system is very complicated. With the previously developed thermodynamic database for the Nb-Ti-Si-Cr system,[9] and the present algorithm for calculating 2D sections of multicomponent liquidus surfaces, we were able to identify how Cr addition can affect the solidification microstructure. Figure 7(a) shows the calculated 2D section of the Nb-Ti-Si-Cr liquidus projection with Cr fixed at 5 at.%. This section has similar phase relationships to that in the metal-rich region of the Nb-Ti-Si ternary system. However, one distinct feature in Fig. 7(a) is the smaller Nb_3Si primary phase region in the Nb-Ti-Si-Cr system compared with that in Fig. 2 for the Nb-Ti-Si system. Figure 7(b) shows the calculated 2D section of Nb-Ti-Si-Cr liquidus projection at 10 at.% Cr, in which the Nb_3Si primary phase region completely disappears at the Nb-rich region. Direct eutectic solidification occurs between (Nb) and αNb_5Si_3 in the Nb-Ti-Si-Cr liquidus projection with 10 at.% addition of Cr. This calculation can explain the experimental observation. In addition, these calculations can identify additional alloys that experience eutectic solidification to form (Nb) and αNb_5Si_3 composites. This method can be used in the study of higher-order multicomponent systems. For example, we

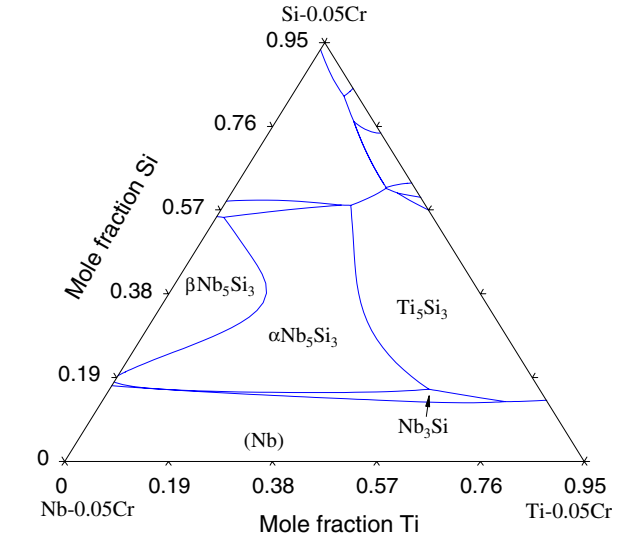

(a)

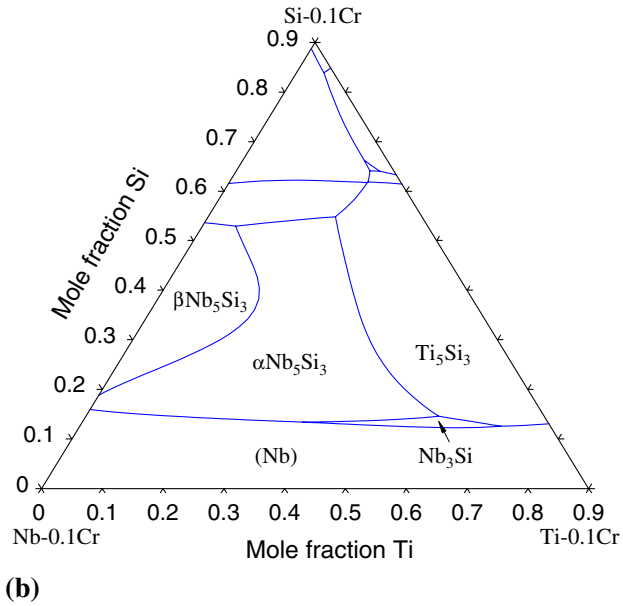

(b)

Fig. 7 Calculated 2D sectional liquidus projections for quaternary Nb-Ti-Si-Cr. (a) Section for 5%Cr: (Y:Si-0.05Cr)-(O:Nb-0.05Cr)-(X:Ti-0.05Cr). (b) Section for 10%Cr: (Y:Si-0.1Cr)-(O:Nb-0.1Cr)-(X:Ti-0.1Cr)

have applied the 2D sectional liquidus projection algorithm to systems with more than five components.

6. Discussions and Conclusions

Two-dimensional sections of liquidus projections are useful for understanding the solidification microstructure of multicomponent systems, identifying the effect of the addition of one or more particular alloying elements to the materials, and providing guidance for composition selection in alloy design and optimization of processing parameters.

However, in 2D sections of liquidus projection, only univariant three-phase equilibrium lines can be viewed. Phase equilibrium with more than four phases usually cannot be seen in such diagrams, except when the 2D section happens to pass through some special points, as the one shown in Fig. 5. To obtain more information on other types of phase equilibria, other diagrams must be calculated.

A 2D sectional liquidus projection is different from a 2D sectional phase diagram in a composition-temperature space. The difference is due to projection. The 2D projection sacrifices a lot of information, and only the univariant phase equilibria in the 2D space are retained.

Even though the algorithm presented here is designed for calculating the 2D sectional liquidus projections for a multicomponent system with more than three components, it can also be used for calculating an ordinary ternary liquidus projection by defining the 2D section as: (1, 0, 0), (0, 1, 0), (0, 0, 1) in the coordinate system (x_A, x_B, x_C). Figure 2 was calculated using this algorithm.

Acknowledgments

Y. Austin Chang wishes to thank the Air Force of Scientific Research (Grant No. FA9550-06-1-0229) and the National Science Foundation (FRG grant no. NSF-DMR-03-09468) for financial support, and Kuo-Chih Chou wishes to thank the financial support from Chinese National Natural Science Foundation (No. 50774004).

References

1. F.N. Rhines, *Phase Diagrams in Metallurgy*, McGraw-Hill, New York, 1956
2. S.-L. Chen, W. Cao, Y. Yang, F. Zhang, K. Wu, Y. Du, and Y.A. Chang, Calculation and Application of Liquidus Projection, *Rare Metals*, 2006, **25**(5), p 532-537
3. S.-L. Chen, S. Daniel, F. Zhang, Y.A. Chang, X.-Y. Yan, F.-Y. Xie, R. Schmid-Fetzer, and W.A. Oates, The PANDAT Software Package and Its Application, *CALPHAD*, 2002, **26**(2), p 175-188
4. S.-L. Chen, F. Zhang, S. Daniel, F.-Y. Xie, X.-Y. Yan, Y.A. Chang, R. Schmid-Fetzer, and W.A. Oates, Calculating Phase Diagrams Using PANDAT and PanEngine, *JOM*, 2003, **55**(12), p 48-51
5. B.P. Bewlay, M.R. Jackson, and P.R. Subramanian, Processing High-Temperature Refractory-Metal Silicide in-Situ Composites, *JOM*, 1999, **51**(4), p 32-36
6. B.P. Bewlay, M.R. Jackson, and H.A. Lipsitt, The Balance of Mechanical and Environmental Properties of a Multi-Element Niobium-Niobium Silicide-Based in Situ Composite, *Metall. Mater. Trans. A*, 1996, **27A**(12), p 3801-3808
7. M.R. Jackson, B.P. Bewlay, R.G. Rowe, D.W. Skelly, and H.A. Lipsitt, High-Temperature Refractory Metal-Intermetallic Composites, *JOM*, 1996, **48**(1), p 39-44
8. M.G. Mendiratta, J.J. Lewandowski, and D.M. Dimiduk, Strength and Ductile-Phase Toughening in the Two-Phase Niobium/Niobium Silicide (Nb5Si3) Alloys, *Metall. Trans.*, 1991, **22A**(7), p 1573-1583
9. Y. Yang, B.P. Bewlay, S.-L. Chen, and Y.A. Chang, Application of Phase Diagram Calculations to Development of New Ultra-High Temperature Structural Materials, *Trans. Nonferrous Met. Soc. China*, 2007, **17**(6), p 1396-1404